

Journal of Turbulence



ISSN: (Print) (Online) Journal homepage: www.tandfonline.com/journals/tjot20

Theory and simulations of confined periodic turbulence

Philippe R. Spalart & Michael S. Dodd

To cite this article: Philippe R. Spalart & Michael S. Dodd (03 May 2024): Theory and simulations of confined periodic turbulence, Journal of Turbulence, DOI: 10.1080/14685248.2024.2342265

To link to this article: https://doi.org/10.1080/14685248.2024.2342265

	Published online: 03 May 2024.
	Submit your article to this journal $oldsymbol{oldsymbol{\mathcal{G}}}$
ılıl	Article views: 39
Q ^L	View related articles 🗗
CrossMark	View Crossmark data 🗷





Theory and simulations of confined periodic turbulence

Philippe R. Spalart^a and Michael S. Dodd^{b,c}

^aBoeing Commercial Airplanes, Woodinville, WA, USA; ^bCenter for Turbulent Research, Stanford University, Stanford, USA; ^cWilliam E. Boeing Department of Aeronautics & Astronautics, University of Washington, Seattle, USA

ARSTRACT

Confined Periodic Turbulence (CPT) is numerical homogeneous turbulence with periodic conditions, over an extended time until the eddy size is only limited by the period L. With large or infinite Reynolds number, this allows a self-similar decaying state with a constant spectrum shape and turbulent kinetic energy k asymptotically equal to $C_{CPT}L^2/t^2$ where t is time and C_{CPT} is a constant, as predicted by Skrbek & Stalp. This setting may provide a long inertial range for a given resolution and is free of inputs such as initial spectra or forcing devices. Outside the viscous range, it generates the same spectra as the Linear Forcing proposed by Lundgren and exercised by Rosales & Meneveau. We conduct DNS, with the viscosity artificially decreasing in time to keep the Reynolds number $Re \equiv L\sqrt{k}/\nu$ approximately constant, and LES at infinite Reynolds number, with resolution 1024³. The solutions indeed lose memory of initial conditions. Both agree well with Rosales & Meneveau and with the L^2/t^2 conjecture although with modulations; C_{CPT} is about 0.5. Kovasznay's extension of Kolmogorov's theory, based on the local energy-transfer rate across wavenumbers, predicts the spectrum well even for intermediate wavenumbers, with the Kolmogorov constant C_K at 1.65.

ARTICLE HISTORY

Received 29 January 2024 Accepted 4 April 2024

KEYWORDS Isotropic turbulence

1. Introduction

The simulation of homogeneous isotropic turbulence has been a central part of the numerical study of turbulence by DNS and LES, partly because of its fundamental stature and partly because of the convenience of periodic boundary conditions. The classical approach, in numerical and in experimental work, is to design a domain appreciably larger than the energy-containing eddies; ideally, many copies of these eddies are present in the domain, and its size L is irrelevant to the results. In the search for numerically pure simulations, there is a grid convergence as the grid spacing Δx and time step Δt tend to 0, and a domain convergence as $L \to \infty$. In periodic simulations, this can be ensured in one of two ways. In decaying-turbulence simulations, an initial flow field in which the energetic eddies are much smaller than the domain is created, and the simulation run only as long as the scale of the dominant eddies has not shifted too close to the domain size. In forced-turbulence simulations, normally the forcing is applied to wavenumbers removed from the fundamental wavenumber of the domain, namely, $k_0 \equiv 2\pi/L$. In both cases, a simulation in which the energy peak moves close to k_0 would be considered tainted. In contrast some simulations extend the forcing, or negative viscosity, all the way to zero wavenumber [1,2], in which case the energy peak is in fact at k_0 (depending on minor details of how the wave-vectors are grouped), much like what will happen in our simulations herein presented.

The classical setting with a peak wave-number of the turbulent activity appreciably larger than k_0 is a careful one, but it has drawbacks. Often, there is little interest in the spectrum 'to the left' of the peak, the interest being in the universal flow features, namely the energy cascade and the small scales. In decaying turbulence, that region of the spectrum is largely arbitrary, for instance, it can be made proportional to k^4 as advocated by Batchelor but, in our opinion, without a fully rigorous reason for that. There are arguments in favour of the power 2 rather than 4, especially from Saffman, and experiments for grid-generated turbulence seem to be close to 3. We agree with many of the points made by Skrbek and Stalp [3] in this respect. In forced turbulence, we conjecture that the low end of the spectrum is sustained by triadic combinations of the forced modes, which is not a physically transparent process. We therefore contend that while a simulation which 'saturates' the domain size so that the turbulence is strongly confined does have unnatural features, these are not unquestionably worse than the unnatural features of the two classical types. Compared with cases forced down to k_0 instead of over a wave-number band, there is no deep difference. A simulation which simply saturates the box has the advantage of simplicity and (statistical) uniqueness, compared with initial condition and forcing schemes which get somewhat complex and non-unique. It may well offer the longest inertial range for a given resolution; however, the flow is not stationary, which brings up questions that are addressed below. An unfortunate aspect is that CPT has no experimental counterpart (for the lower wavenumbers).

At very large Reynolds numbers, the CPT setting allows a self-similar decaying state with a simple theoretical prediction for the turbulent kinetic energy k, namely an inverse-square time dependence. If the Reynolds number is finite, the decay will not be self-similar, unless the viscosity is made to decrease as $v(t) = C_{CPT}^{1/2} L^2/(t Re)$ where Re was chosen arbitrarily. We adopted this approach here for the DNS. In contrast, the molecular viscosity of the LES was set to zero, so that the flow has an infinite Reynolds number. Running without any molecular viscosity appears to be a new practice, but we would defend it also in conventional non-confined simulations, arguing that in a true LES the grid spacing is far larger than the Kolomogorov scale: $\Delta x \gg \eta$. In this setting, a well-resolved LES (meaning one with a large number of points within L) will approach the pure value of the C_{CPT} constant, and the DNS will produce a function $C_{CPT}(Re)$ which asymptotes to the infinite-Re value. According to Kolmogorov 41 theory, it would proceed like an inverse square root, that is, $C_{CPT}(Re) = C_{CPT}(\infty) - C_{VR}Re^{-1/2}$ where $C_{VR} \approx 2.5$ based on DNS results for the Kolmogorov viscous range and assuming a Kolmogorov constant equal to 1.7 [2,4,5].

In both cases, there is every reason to expect a normal energy cascade towards small scales inside CPT, so that studies of the inertial and viscous ranges of the spectrum will be unaffected. With proper scaling, the results can also be averaged in time, which is not possible or at least quite difficult for classical decaying (or even strained or sheared) turbulence. As mentioned in the abstract, the large scales of motion are not exactly isotropic, but that does not invalidate the energy cascade, and this issue may affect the simple forcing schemes also.

An original line of work is that initiated by Lundgren [6] and continued by Rosales and Meneveau [7], Bassenne and Urzay [8], Palmore Jr and Desjardins [9]; it is also used by Piomelli et al. [10]. The 'Linear Forcing' is uniform, simply adding to the momentum equation a term proportional to the velocity perturbation u', multiplied by a coefficient A which is an inverse time. It can be applied in Fourier or real space. We will show that our decaying solutions and their forced solutions bear a simple relationship, except for the viscous term. They essentially produce the same turbulence. This arguably gives an interesting angle from which to view the linearly-forced solutions, an insight Lundgren himself clearly hinted at on p. 464 [6]. The viscous term can be handled with an artificial decrease of the viscosity, leading to a complete equivalence, as will be shown in Section 3.

We agree with most of the points made by Rosales & Meneveau about linearly-forced turbulence [7], but not with the description of the turbulence as simply isotropic. The largest eddies are not quite isotropic because the periodicity operator is not spherical. Another explanation is that the two-point correlations must satisfy a Neumann condition on the surface of the cube (if the first point is in its centre), by symmetry. This is not compatible with isotropy, which demands that the correlations be functions only of distance. In non-confined turbulence, the correlations have died down to very small levels for separations of order L, so that the conflict is very weak; this is not the case in CPT, in which the correlation at a distance L/2 in the x direction is still of the order of 0.15 as will be shown.

We also believe Rosales & Meneveau did not insist quite clearly enough on the confinement effects (although in the end they did refer to the energy-containing scales being 'contaminated by finite domain-size effects'), and that the apparently wider inertial range they obtained with low-k (i.e. non-uniform) forcing than with linear forcing is a little artificial (their Figure 12). Finally, we have to note that outside homogeneous turbulence, linear forcing is not as simple as it may seem, because it would require advanced knowledge of the averaged flow field, to calculate u' (in homogeneous turbulence, this average is zero). Still, this line of work is highly relevant to the present one.

The shorter expression Confined Turbulence would, unfortunately, conflict with its prior use by Johnsen et al. [11] since they are studying turbulence confined by viscous walls. This is a more complex situation, and no relation between the two types of flows is expected. Confined Periodic Turbulence seems descriptive.

These considerations constitute the motivation for a study, including a variety of initial conditions and, of course, the difference between DNS and LES. Our primary purpose here is to propose Confined Periodic Turbulence as a valid tool to study the energy cascade and to verify the postulated scaling laws. There is also a lesson in the connection with Linear Forcing. More studies focused on the cascade may come later if indeed this flow is accepted as relevant by the scientific community of turbulence. In Section 2 we present the analytical correspondence between decaying and linearly-forced solutions. In Section 3 we propose a theory for the spectrum at wavenumbers smaller than those in the fully-inertial range. In Section 4 we outline the numerical method and sub-grid-scale (SGS) model. In Section 5 we present the results, and in Section 6 we present conclusions and an outlook.

2. Relationship to linear forcing

Consider an unforced solution, $\mathbf{u}_1(\mathbf{x}, t_1)$, of the incompressible $(\nabla \cdot \mathbf{u} = 0)$ Navier-Stokes equations written with a time dependent viscosity, $v(t_1)$,

$$\frac{\partial \mathbf{u}_1}{\partial t_1} + \mathbf{u}_1 \cdot \nabla \mathbf{u}_1 = -\nabla p_1 + \nu(t_1) \nabla^2 \mathbf{u}_1. \tag{1}$$

Let T be an arbitrary time scale, and define the fields $\mathbf{u}_2 \equiv (t_1/T)\mathbf{u}_1$ and $p_2 \equiv (t_1^2/T^2)p_1$, as well as the time $t_2 \equiv T \log(t_1/T)$. The two flow fields (1 and 2) have the same domain size L. The Navier-Stokes equations written for \mathbf{u}_2 is

$$\frac{\partial \mathbf{u}_2}{\partial t_2} + \mathbf{u}_2 \cdot \nabla \mathbf{u}_2 = -\nabla p_2 + \frac{t_1}{T} \nu(t_1) \nabla^2 \mathbf{u}_2 + \frac{1}{T} \mathbf{u}_2, \tag{2}$$

in which we recognise the Linear Forcing term $A\mathbf{u}_2$ [6], with A=1/T. If, further, $t_1v(t_1)$ is constant, \mathbf{u}_2 satisfies Lundgren's Equations (2), (3) with the constant viscosity $v_2 = (t_1/T)v(t_1)$.

This demonstrates a direct relationship between solutions of the unforced equations with viscosity scaling like $1/t_1$, and linearly forced equations with constant viscosity. The two sets of equations give fields which are proportional to each other, in domains of the common size L.

In both systems, the forcing or time evolution has the same inverse time scale A or $1/t_1$ across all length scales of the turbulence, and the small eddies of size l have shorter time scales proportional to $(l^2/\epsilon)^{1/3}$ where ϵ is the dissipation rate. As a result, the small eddies are less sensitive to A or t_1 than the large scales are. This is a classical argument in favour of isotropy and universality of the small eddies.

In our simulations of CPT, the Linear Forcing simulations have a constant A and by dimensional analysis gives, $A = C_{LF}\sqrt{k_2}/L$ with C_{LF} a universal constant, while the decaying simulations have $k_1 = C_{CPT}L^2/t_1^2$ as mentioned before. When $t_1 = T$, we have $k_1 = k_2 = k$, and this leads to $C_{CPT} = 1/C_{LF}^2$. Rosales & Meneveau's [7] Cases 3a-3c have, in their units, $k \approx 0.67$ when A = 0.2 and $L = 2\pi$. Therefore, $C_{LF} \approx 1.5$, implying $C_{CPT} \approx 0.45$, which are in excellent agreement with our numerical results of CPT below.

3. Extension of Kolmogorov's theory to wavenumbers smaller than the pure inertial range

Kolmogorov's 1941 theory [12] revolves around a single energy-transfer rate ϵ_{∞} , which dominates the description in the inertial range and viscous range of the spectrum. More generally we can define an energy flux at each wavenumber k, namely the rate of loss of the amount of energy contained in lower wavenumbers, k' < k, produced by the nonlinear term in the momentum equation [13]. The idea of an energy transfer that is fully 'local' in wave space is only an approximation, since wavevector triads exchange energy between the two sides of k over a range of wavenumbers; however, this range is less than an order of magnitude, so that a simple 'local' approximation may have merit, and deserves comparison with simulation results. Davidson [13] surveys similar proposals by Obukhov and others, which could be tested unambiguously with the present type of simulations.

Assume a scaling for the spectrum of the type

$$E(k) = LkF'(kL), \tag{3}$$

where F' is the derivative of F, which itself is a universal function with F(0) = 0 and $\lim_{kL \to \infty} F(kL) = 1$. As the flow lives on, the spectrum has statistical oscillations in the neighbourhood of this distribution, and the oscillations are weak when $kL \gg 1$, because the sample of wavevectors is larger in larger 'shells' (in fact, for kL of order less than 20, the calculation of the three-dimensional energy spectrum is ambiguous because the number of wavevectors is not large enough). The energy up to wave-number k is kF(kL), and k is decaying. Therefore, the energy flux across k towards small scales is

$$\epsilon(k) = -\frac{\mathrm{d}k}{\mathrm{d}t}F(kL). \tag{4}$$

For $kL \gg 1$, this energy flux is close to the full dissipation $\epsilon_{\infty} = -\mathrm{d}k/\mathrm{d}t$ because F approaches 1. Here, we are neglecting viscous dissipation up to k, and considering only the inviscid energy transfer. We are also ignoring the fluctuations in time relative to the exact $1/t^2$ decay, which are discussed below.

A standard inertial range will have

$$E(k) = C_K \epsilon_\infty^{2/3} k^{-5/3} \tag{5}$$

where C_K is the Kolmogorov constant, and we conjecture the same relationship with the local energy transfer rate:

$$E(k) = C_K \epsilon(k)^{2/3} k^{-5/3}. \tag{6}$$

This is our key assumption, and it is not trivial. It is equivalent to that of Kovasznay in 1948 [13,14]. Note that both Kovasznay [14] and Davidson [13] examined its consequences for the spectrum in the viscous range, when $k\eta$ approaches the order of 1 and it begins to deviate downwards from the -5/3 law, and the approximation was only moderately successful. In contrast, our interest is in the deviations of the spectrum at the other end of the pure inertial range, i.e. at wavenumbers smaller than the conventional inertial range. Calling this range 'inertial' is correct in the sense that the viscosity plays no role.

For fully-developed CPT, analytical predictions are possible and are described in detail below. For other types of homogeneous turbulence simulations, analytical forms are usually not available, but the hypothesis can be tested at a given time by accounting for both the time derivative of the kinetic energy contained in wavenumbers smaller than k, and if applicable the rate of forcing over the same range of wavenumbers. Therefore, Equation (6) is a candidate to correct Kolmogorov's simple spectrum for wavenumbers moderately smaller than the pure inertial range.

In CPT, assuming that the turbulence kinetic energy, k, is

$$k = C_{CPT} \frac{L^2}{t^2},\tag{7}$$

then

$$\epsilon_{\infty} = -\frac{\mathrm{dk}}{\mathrm{d}t} = 2C_{CPT} \frac{L^2}{t^3},\tag{8}$$

Using Equations (3), (4), (6), and (7) leads to the following ordinary differential equation for F:

$$C_{CPT}^{1/3}F'(kL) = C_K(2F)^{2/3}(kL)^{-5/3},$$
(9)

whose solution is

$$F = \left[1 - C_K (2C_{CPT})^{-1/3} (kL)^{-2/3}\right]^3. \tag{10}$$



Using (10), the equation for E(k) (3) gives

$$E(k) = 2^{2/3} L k C_K C_{CPT}^{-1/3} \left[1 - C_K (2C_{CPT})^{-1/3} (kL)^{-2/3} \right]^2 (kL)^{-5/3}$$

$$= C_K \epsilon_{\infty}^{2/3} \left[1 - C_K (2C_{CPT})^{-1/3} (kL)^{-2/3} \right]^2 k^{-5/3}, \tag{11}$$

which is compatible with the type assumed above for E(k). The last expression (11) is Kolmogorov's classic $E(k) = C_K \epsilon_{\infty}^{2/3} k^{-5/3}$, but with a correction factor in brackets. These results contain no new adjustable parameters, which allows for a rigorous verification through simulations of CPT. The simulation results of the energy spectrum E(k) can be compared to the derived analytical spectrum Equation (11) or with Equation (4) directly, with

$$\epsilon(k) = -\frac{\mathrm{d}}{\mathrm{d}t} \left(\int_0^k E(k') \, \mathrm{d}k' \right) = -\frac{\mathrm{d}k}{\mathrm{d}t} F(kL). \tag{12}$$

Agreement is not expected towards zero wavenumber, since, from Equations (10) and (11), $\lim_{k\to 0} F(k) =$ $-\infty$ and $\lim_{k\to 0} E(k) = \infty$.

Pao's [15] similarity hypothesis gives

$$E(k) = C_K \epsilon_{\infty}^{2/3} k^{-5/3} \exp\left(-3 \, 2^{1/3} C_K (kL)^{-2/3}\right). \tag{13}$$

We show its results below, but in our opinion, the role of ϵ_{∞} makes it less convincing physically than our proposal for low-to-moderate wavenumbers.

4. Numerical method

4.1. Solver

We performed direct numerical simulation (DNS) and large eddy simulation (LES) to solve the unsteady Navier-Stokes equations for incompressible flow. The computational domain is a cube with periodic boundary conditions in all three spatial directions. The governing equations are discretised in space using the secondorder accurate central difference scheme on uniform staggered grids ranging from 256³ to 1024³ points. The LES is performed using the Smagorinsky model [16] with $C_S = 0.17$. The pressure-correction method is used to advance the solution in time, i.e. the pressure is treated implicitly and obtained by solving the Poisson equation in finite-difference form using a combination of one-dimensional fast Fourier transforms (FFTs) in the x and y direction and specialised Gauss elimination in the z direction [17]. More details about the parallel fast Poisson solver are given in Ref. [18]. Time integration is performed using the second-order Adams-Bashforth scheme. In the DNS (finite Re) cases, the viscosity is decreased in time as $v(t) = C_{CPT}^{1/2} L^2/(t Re)$, where $C_{CPT} = 0.5$. Also, the time step, Δt , is computed as $\Delta t = \Delta x/(40\sqrt{k})$, thus Δt increases in time as k decreases and the integral time scale increases. This results in maintaining the CFL number approximately constant in time.

With regard to the practice of letting the viscosity decay to sustain the Reynolds number, we have shown that it is equivalent to forcing turbulence by keeping the viscosity constant and re-scaling the velocity field such to keep k constant in time. Also, this has similarities with the practice of a negative viscosity or a velocity re-scaling which has been used since Kerr [1], with the crucial difference that the present method does not have a cut-off for the wave-numbers which receive the re-scaling, and thus it has the advantage of avoiding the arbitrary choice of setting a cutoff scale, e.g. for $k/k_0 < 2.5$.

4.2. Initial conditions

We initialise the velocity field with various initial conditions as follows: (i) 2-D Taylor-Green vortex flow [19] (for which a small perturbation is introduced to break the initial symmetries; case 2), (ii) 3-D isotropic turbulence with initial energy spectrum according to the model spectrum by Pope [20] (Cases 3-8), and (iii) uniformly distributed random numbers between -1 and 1, and projected to satisfy the divergence-free constraint (Case 1). These three approaches yield initial energy spectra $(E(\kappa))$ in which the majority of the

Table 1. Summary of the simulation cases that were studied.

Case	N^3	Туре	Initial conditions	Re
1	256 ³	DNS	random numbers	3000
2	256 ³	DNS	Taylor-Green vortex	3000
3	256 ³	DNS	isotropic turbulence	3000
4	256 ³	LES	isotropic turbulence	∞
5	256 ³	DNS	isotropic turbulence	1500
6	512 ³	DNS	isotropic turbulence	8000
7	512 ³	LES	isotropic turbulence	∞
8	1024 ³	LES	isotropic turbulence	∞

Note: The LES cases use the Smagorinsky model with $C_S = 0.17$ and the molecular viscosity is set to zero.

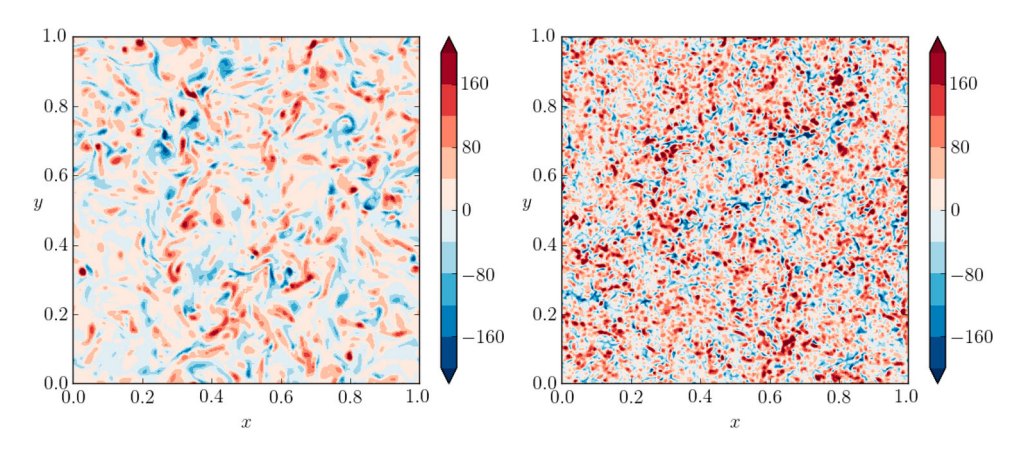


Figure 1. Normalised z-vorticity contours $(\omega_z L/\sqrt{k})$ in an x-y plane in a mature flow field. Left, Case 3 (DNS, Re = 3000); Right, Case 4 (LES, Re $= \infty$).

energy is concentrated in the low, intermediate, and high wavenumbers, respectively. The simulations are run for approximately 50 integral time scales. The integral time scale is defined as $\tau_{\ell} = \ell/u_{\rm rms}$, where ℓ is the longitudinal integral length scale. We note that for $t \gg 0$, ℓ is roughly invariant in time with a mean value $\ell = 0.15$ (Table 1).

5. Results

5.1. Flow visualisations

We begin by showing visualisations of Confined Periodic Turbulence (CPT) obtained from our numerical simulations. Figure 1 shows vorticity contours for Cases 3 and 4. The vorticity contours appear typical of periodic simulations and show no indication of being dominated by an eddy or a few eddies of size close to L. In other words, the confinement is far from blatant in physical space (compare with the Taylor-Green initial condition, for instance). In contrast, a two-dimensional simulation would evolve to a very small number of eddies. The velocity contours in Figure 2, being less dominated than vorticity contours by small scales of motion, are more suggestive of rather long waves, but the confinement is still not obvious. Arguably, the simulation contains a large enough number of eddies, evolving independently of each other. This is physically satisfactory. The integral length scale of the turbulence is about 0.4L; in that sense, the confinement is unmistakable. With the same 256³ resolution but a higher Reynolds number, the large-eddy simulation (Case 4) naturally produces much finer grain than the DNS (Case 3), which will be reflected in the spectra, below.

5.2. Isotropy considerations

Figure 5 shows the longitudinal two-point correlations in Case 4 for the x direction, and in the direction oblique between the x and y axes, that is,

$$f_1(r,t) = \frac{\langle u_1(\mathbf{x} + r\mathbf{e}_1, t)u_1(\mathbf{x}, t)\rangle}{\langle u_1^2 \rangle}, \quad f_{12}(r,t) = \frac{\langle u_{12}(\mathbf{x} + r\mathbf{e}_{12}, t)u_{12}(\mathbf{x}, t)\rangle}{\langle u_{12}^2 \rangle}.$$
 (14)

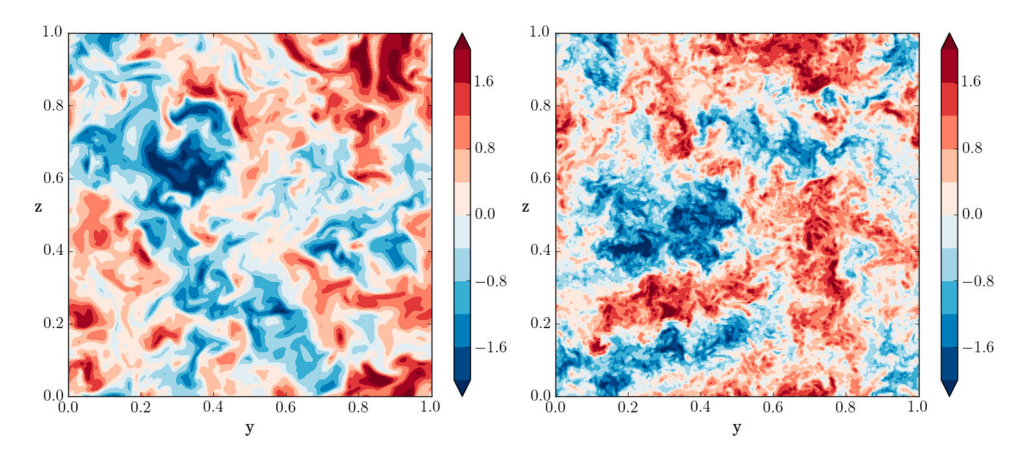


Figure 2. Normalised u_1 -velocity contours (u_1/\sqrt{k}) in an x-y plane in a mature flow field. Left, Case 3; Right, Case 4.

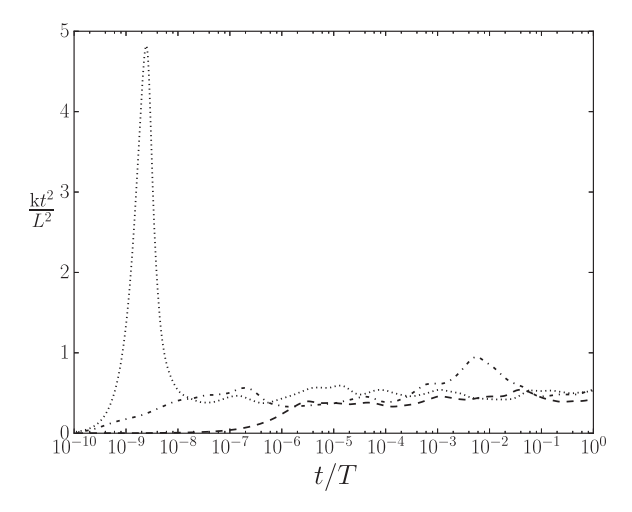


Figure 3. Time evolution of the pre-multiplied turbulent kinetic energy, with various initial conditions for Re = 3000 on a 256^3 mesh. ---, random numbers (Case 1); $-\cdot-$, isotropic turbulence (Case 3); \cdots , Taylor-Green vortex (Case 2).

where $u_{12} \equiv (u_1 + u_2)/\sqrt{2}$ and $\mathbf{e}_{12} \equiv (\mathbf{e}_1 + \mathbf{e}_2)/\sqrt{2}$. The functions f_1 and f_{12} were time averaged for 10 flow realisations evenly spaced over $t/T = [10^{-7}, 10^0]$, where T is the final time of the simulation. The two curves coincide for small separations, and depart decidedly for larger separations, fully confirming the expectation that in CPT the small scales are isotropic, and the large scales are mildly anisotropic. This issue was mentioned in Section 1.

5.3. Turbulent kinetic energy

We now test the hypothesis of a $1/t^2$ behaviour for k. Figure 3 presents kt^2/L^2 versus time for various initial conditions (Cases 1–3). As discussed in the Introduction, this quantity is expected to equal C_{CPT} in the long run. This normalisation and a logarithmic axis for time make the presentation equivalent to the natural presentation for linearly forced turbulence; in other words, the right half of the figure may be viewed as 'well-developed.' The simulations are long enough that a virtual origin of time is not necessary. The figure is quite in favour of the theory, and in particular a large surge is seen with the Taylor-Green initial condition (Case 2) leaves no permanent effect. The 'apparent' C_{CPT} oscillates between roughly 0.35 and 0.7. These modulations are unexpectedly strong, just like those observed by Rosales & Meneveau; they also had a factor of approximately 2, peak-to-peak, if we include the rare excursions in their long simulations. The physics will be discussed below.

Figure 4 again presents kt^2/L^2 versus time, to explore the effect of resolution and Reynolds number (Cases 3–6). Increasing resolution at fixed Reynolds number predictably increases the TKE, but by a small amount



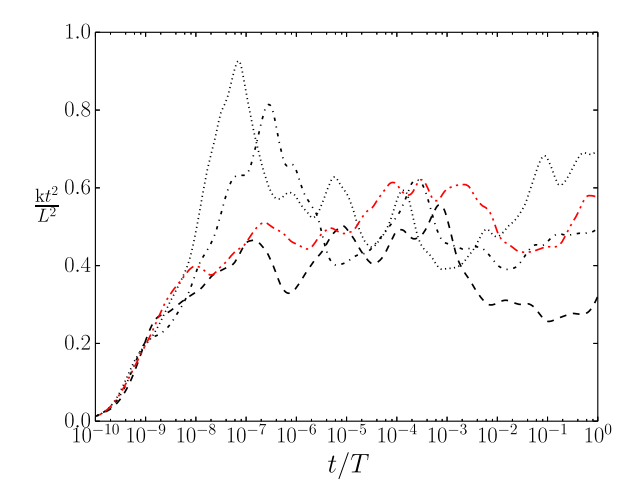


Figure 4. Time evolution of the pre-multiplied turbulent kinetic energy, with different Reynolds numbers and resolutions, in DNS: --, 256³, Re = 1500 (Case 5); --, 256³, Re = 3000 (Case 3); -- 512³, Re = 8000 (Case 6); and in LES: --- 256³, $Re = \infty$ (Case 4).

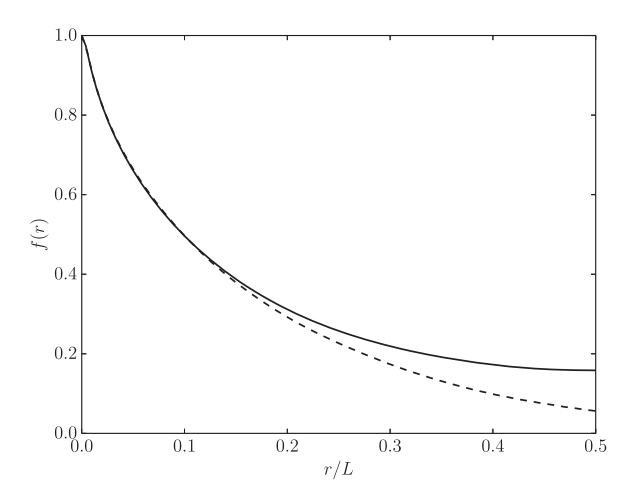


Figure 5. Time-averaged two-point velocity correlation for Case 4. –, f(r) computed in a coordinate direction (\mathbf{e}_1); – – –, f(r)computed in a diagonal direction ($\mathbf{e}_1 + \mathbf{e}_2$).

with the resolutions used here. The 256³ simulation had $\Delta x = 2\eta$ where $\eta = (v^3/\epsilon)^{1/4}$ is the Kolmogorov length scale and ϵ is the dissipation rate. These are typical values. The velocity-derivative skewness is about -0.48, which is accurate. The modulations are very similar to those in the other set of simulations, thus confirming the universal behaviour of mature solutions. The slope of the modulations is of interest. Figure 4 shows that the highest slope $d(\log(kt^2))/d(\log(t))$ is of the order of ± 0.4 . The inviscid evolution would make this slope equal +2. In that sense, the time evolution term (which would be the forcing term in Lundgren's setting) is out of balance with the dissipation by about 20% in alternating directions; this is significant, but not large. This is confirmed by Figure 6, showing the normalised dissipation versus normalised kinetic energy in Case 4. They satisfy

$$\frac{\mathrm{d}(kt^2/L^2)}{\mathrm{d}(\log t)} = \frac{2kt^2}{L^2} - \frac{\epsilon t^3}{2L^2}$$
 (15)

and therefore, the orbits are travelled counter-clockwise, and when the two quantities are equal, on the dashed line, the orbit is vertical (i.e. $d(kt^2/L^2)/dt = 0$). The initial transient was removed until the curve started inside the 'visible attractor.' The correlation between energy and dissipation is very strong and positive. Other figures show that the dissipation typically lags by 0.5 units in log t. To gain perspective, note that $e^{2/3}$ which is part of the Kolmogorov formula varies by about $\pm 25\%$ at the extremes (since ϵ itself varies by about $\pm 40\%$). The average value of the function $f(x) \equiv x^{2/3}$ over the interval 0.6 < x < 1.4 is 0.994, in other words, the

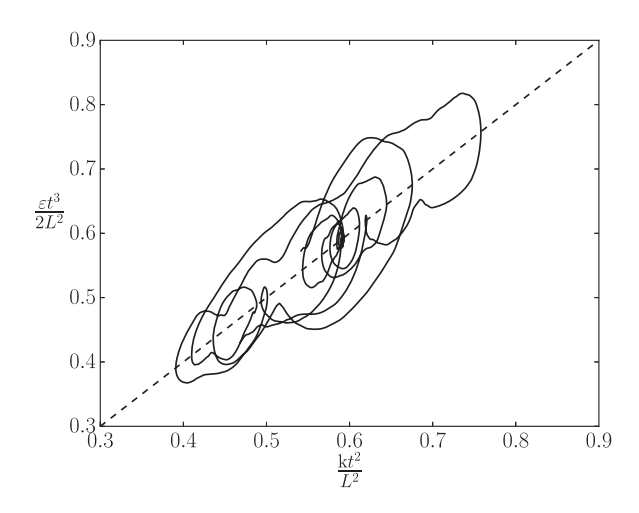


Figure 6. Trace of the normalised kinetic energy and dissipation in LES: – 256^3 , $Re = \infty$ (Case 4).

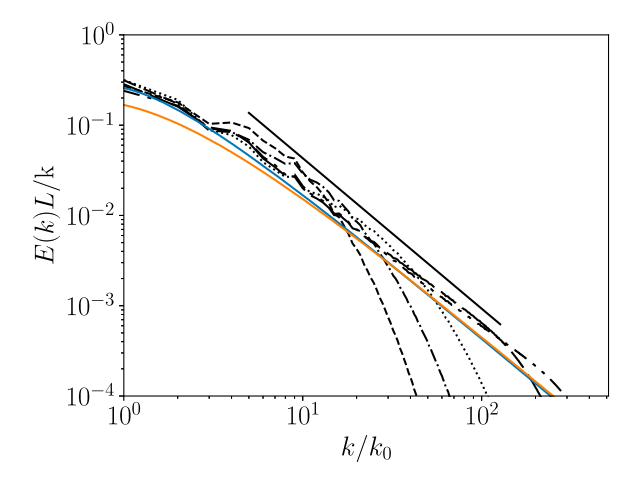


Figure 7. Time-averages of the turbulent kinetic energy spectra normalised by L and L in DNS cases, L cases, L

function is not strongly convex over this range. Therefore, the impact on a calculation of the Kolmogorov constant C_K , for instance, would be negligible.

Figure 6 demonstrates the sustained excursions of energy and dissipation but does not in itself represent *deterministic* chaos the way the Lorenz attractor does, because the two quantities are not subject to two ordinary differential equations (if they were, the orbits would not cross). There is only (15). It is very likely the entire system of equations of the LES has a strange attractor, but this figure is only a symptom of it, of which the physical meaning should not be exaggerated since it is dominated by the confinement effect.

5.4. Spectra

Figure 7 shows energy spectra for DNS with various resolutions and Re values (Cases 3, 5, and 6), and for LES for 1024^3 mesh and $Re = \infty$ (Case 8). The spectra are normalised by k, and then time averaged over the last 12.8 turnover times. The dissipation ϵ_{∞} was calculated by spatially averaging the product of the molecular or eddy viscosity and the square of the strain tensor. The comparison with (11) is quite favourable. The theory deviates from the -5/3 spectrum for k/k_0 below roughly 15, and the simulated spectra with higher Reynolds numbers have a very similar trend, even following it down to the fundamental wavenumber k_0 , where the correction relative to an extrapolation of the -5/3 spectrum is a factor of almost 3 which is considerable.

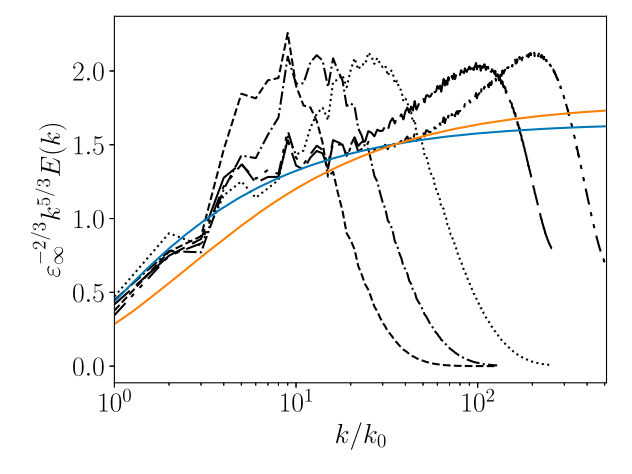


Figure 8. Time-averages of the pre-multiplied energy spectra in DNS cases, --, 256³, Re=1500 (Case 5); $-\cdot-$, 256³, Re=3000 (Case 3); \cdots , 512³, Re=8000 (Case 6); LES cases, --, 512³, $Re=\infty$ (Case 7), $-\cdot\cdot-$, 1024³, $Re=\infty$ (Case 8); - (blue) Equation (11); - (orange) Equation (13).

The agreement with Rosales & Meneveau is very good, including for instance the dip of the spectrum at $k/k_0 = 3$, followed by a rise at 4. As expected the two systems of equations, namely linear forcing and free decay, produce the same flow fields.

Figure 8 shows the time-averaged spectrum pre-multiplied by $\kappa^{5/3}$, which allows the use of a linear vertical scale and is therefore much more discriminating. This confirms the close agreement with (11): the agreement on the shape of the spectrum is surprisingly good even towards very small wavenumbers. In addition, the response of LES to grid refinement is fully consistent with the theory, the upwards spectral bump near $k=0.4k_{\rm max}$ simply sliding to higher wavenumbers and following the upward trend of (11) while the spectra are virtually identical up to wavenumber around $10k_0$. We consider this spectral bump as undesirable, and in hindsight would lower the value of the Smagorinsky constant to try and extend the -5/3 range, but we lost access to the computing facility. Thus Kovasznay's approximation appears to have more merit in this lower part of the spectrum than it does in the viscous range, and to be a powerful tool when attempting to determine C_K accurately, say within an uncertainty of 0.05.

Rosales & Meneveau compared linearly forced turbulence and turbulence forced only for wavenumbers satisfying $kL < 4\pi$, and concluded that the latter type of forcing allowed a longer conventional inertial range for the same resolution. The integral length scale of the turbulence was near 0.4L with linear forcing, instead of 0.2L with low-k forcing. This is significant, but it must be recalled that forcing for all wavenumbers less than $kL < 4\pi$ until a statistically steady state is reached also produces confined turbulence. The classical 'large domain' approach forces only over a range of wavenumbers that does not extend down to zero, and then the integral length scale of the turbulence will be markedly smaller again, thus shortening the inertial range. The spectra presented here suggest that the 'pure' inertial range is reasonably wide, extending down to k/k_0 of the order of 15 when viewed on a logarithmic scale. The linear scale is far more demanding if a precise value of C_K is the objective, suggesting a limit closer to 100 than to 15. In contrast, if (11) is accepted, then the extended inertial range is quite wide, and for instance, a calculation of the Kolmogorov constant C_K might attempt a visual fit down to k/k_0 of the order of 5.

6. Outlook

We have attempted to present what we call Confined Periodic Turbulence with a little more clarity, qualifications, and understanding than the literature had, and to argue that it offers a convenient and correct setting to study the energy cascade and other physics of the medium- and small-scale eddies in homogeneous turbulence. CPT was shown to be accessible either in the setting of Linear Forcing due to Lundgren [6] and well exercised to a stationary state by Rosales and Meneveau [7], or a new setting of long natural decay, possibly with artificially decaying viscosity in a DNS, or zero viscosity if using LES. In fact, with zero viscosity, the fully-developed flow has no physical non-dimensional parameters at all (only numerical parameters), and no

dependence on initial conditions (provided of course they contain the seeds of turbulence); we view these facts as quite favourable for any theoretical study. The problem definition could not be simpler, and comparisons between research groups are rigorous. The time-averaged spectrum is a universal function of turbulence (for which the results of Rosales & Meneveau and ours agreed quite well), just like C_{CPT} is a universal constant. The only parameters of the numerical simulation are its resolution, say 512³ grid points and a set CFL number, and of course the type of discretisation in space and time, in addition of course to the SGS model. Conversely, the study of CPT is possible only in numerical simulations, but these are now a very well-accepted fundamental research tool especially for free turbulent flows.

The quantitative agreement with results in the literature is quite good for the key constants, AL/\sqrt{k} in a forced simulation and C_{CPT} in a decaying one, and also for the spectra. We proposed a plausible extension of the Kolmogorov 1941 law for the spectrum, almost identical to Kovasznay's but free of adjustable parameters other than the Kolmogorov Constant, and the simulation results followed it well, suggesting that an 'extended' inertial range with a non-uniform energy-transfer rate is present. This approximation is based on a non-trivial assumption of 'locality' of the energy transfer in wavenumbers space, and the simple criterion we used applies only to the types of simulated turbulence considered here. However, Equation (6) has no such limitation and could be tested in any simulation of isotropic or nearly-isotropic turbulence, steady or not. We believe $\epsilon(k)$ is a well-defined quantity, and in fact that assuming the relationship in (6) is very consistent with Kolmogorov's thinking.

The simulations confirmed the sizable modulations of the turbulent kinetic energy around its long-term trend, as found by Rosales & Meneveau. We argued that these may not be undesirable, or contrary to the intermittency found in all turbulent flows (although not akin to the alternance of turbulent and non-turbulent patches at the edge of turbulent shear layers). According to (10), 50% of the energy is contained in a sphere of radius $k/k_0 = 4$ in spectral space, which contains almost 300 wave-vectors. Thus, it is not a sample of only a few Fourier modes, yet their collective energy sustains significant modulations. There is a clear stable feedback mechanism between energy and dissipation, as seen in Figure 6. The attractor of the solution, even in CPT which might have been expected to tend to relatively simple behaviour, is complicated indeed.

Acknowledgments

This work was facilitated through the use of advanced computational, storage, and networking infrastructure provided by the HYAK supercomputer system at the University of Washington. The authors thank Dr A. Wray, Dr C. Mockett, and Prof. P. Davidson for their instructive comments.

Data availability statement

The time-series data used for the line graphs is available upon reasonable request. The three-dimensional flow field data used for Figures 1 and 2 is not available due to cessation of access to the HYAK storage system.

Disclosure statement

No potential conflict of interest was reported by the author(s).

References

- [1] Kerr RM. Higher-order derivative correlations and the alignment of small-scale structures in isotropic numerical turbulence. J Fluid Mech. 1985;153:31-58. doi: 10.1017/S0022112085001136
- [2] Ishihara T, Gotoh T, Kaneda Y. Study of high-Reynolds number isotropic turbulence by direct numerical simulation. Annu Rev Fluid Mech. 2009;41:165-180. doi: 10.1146/fluid.2009.41.issue-1
- [3] Skrbek L, Stalp SR. On the decay of homogeneous isotropic turbulence. Phys Fluids. 2000;12:1997-2019. doi: 10.1063/1.870447
- [4] Sreenivasan KR. On the universality of the Kolmogorov constant. Phys Fluids. 1995;7:2778–2784. doi: 10.1063/1.86
- [5] Yeung PK, Zhou Y. Universality of the Kolmogorov constant in numerical simulations of turbulence. Phys Rev E. 1997;56:1746–1752. doi: 10.1103/PhysRevE.56.1746
- [6] Lundgren TS. Linearly forced isotropic turbulence. In: Annual Research Briefs. Stanford: Center for Turbulence Research; 2003. p. 461-473.



- [7] Rosales C, Meneveau C. Linear forcing in numerical simulations of isotropic turbulence: physical space implementations and convergence properties. Phys Fluids. 2005;17:Article ID 095106. doi: 10.1063/1.2047568
- [8] Bassenne M, Urzay J, Park GI, et al. Constant-energetics physical-space forcing methods for improved convergence to homogeneous-isotropic turbulence with application to particle-laden flows. Phys Fluids. 2016;28:Article ID 035114. doi: 10.1063/1.4944629
- [9] Palmore Jr JA, Desjardins O. Technique for forcing high reynolds number isotropic turbulence in physical space. Phys Rev Fluids. 2018;3:Article ID 034605. doi: 10.1103/PhysRevFluids.3.034605
- [10] Piomelli U, Rouhi A, Geurts BJ. A grid-independent length scale for large-eddy simulations. J Fluid Mech. 2015;766:499-527. doi: 10.1017/jfm.2015.29
- [11] Johnsen E, Movahed P, Dowling D. A numerical study of turbulence in boxes with no-slip walls and of varying volume-to-surface ratios. In: 45th AIAA Fluid Dynamics Conference, Dallas, TX; 2015. p. 3081.
- [12] Kolmogorov AN. The local structure of turbulence in incompressible viscous fluid for very large reynolds numbers. In: Doklady Akademii Nauk SSSR; Vol. 30. JSTOR; 1941. p. 301–305.
- [13] Davidson PA. Turbulence: an introduction for scientists and engineers. Oxford, UK: Oxford University Press; 2004.
- [14] Kovasznay LSG. The spectrum of locally isotropic turbulence. Phys Rev. 1948;73:1115–1116. doi: 10.1103/Phys Rev.73.1115
- [15] Pao YH. Structure of turbulent velocity and scalar fields at large wavenumbers. Phys Fluids. 1965;8:1063-1075. doi: 10.1063/1.1761356
- [16] Smagorinsky J. General circulation experiments with the primitive equations: I. the basic experiment*. Monthly Weather Rev. 1963;91:99-164. doi: 10.1175/1520-0493(1963)091<0099:GCEWTP>2.3.CO;2
- [17] Schmidt H, Schumann U, Volkert H. Three dimensional, direct and vectorized elliptic solvers for various boundary conditions. Institution DFVLR-Mitt; 1984. (type Rep. number 84-15).
- [18] Dodd MS, Ferrante A. A fast pressure-correction method for incompressible two-fluid flows. J Comput Phys. 2014;273:416-434. doi: 10.1016/j.jcp.2014.05.024
- [19] Taylor GI. On the decay of vortices in a viscous fluid. Philos Mag. 1923;XLVI:671-674. doi: 10.1080/147864423086
- [20] Pope SB. Turbulent flows. Cambridge, UK: Cambridge Univ. Press; 2000.